

Exploratory study on the rheological behaviour of 3D printable mortars incorporating fine recycled concrete aggregates (FRCA)

Eduardo KloECKner Sbardelotto^{1,2*}, *Manuel Gomes Vieira*², *Karyne Ferreira dos Santos*³, *Samuel Pereira dos Santos*³ and *Berenice Martins Toralles*¹

^{1*} Programa de Pós-Graduação em Engenharia Civil (PGECiv), Universidade Estadual de Londrina (UEL), Rodovia Celso Garcia Cid, PR-445, km 380, 86057-970, Londrina, PR, Brazil; eduardoklsb@gmail.com (E.K.S.); toralles@uel.br (B.M.T.)

² Laboratório Nacional de Engenharia Civil (LNEC), Av. do Brasil, 101, 1700-066 Lisbon, Portugal; mvieira@lnec.pt (M.G.V.)

³ Sustainable Construction Materials Association (C5Lab), Edifício Central Park, Rua Central Park 6, 2795-242 Linda-a-Velha, Portugal; ksantos@c5lab.pt (K.F.S.); ssantos@c5lab.pt (S.P.S)

Abstract. This study investigates the rheological behaviour of 3D-printable mortars incorporating fine recycled concrete aggregates (FRCA), focusing on the influence of 25% and 50% FRCA substitution on key rheological parameters, such as flow spread, penetration resistance, shear stress, and yield stress over time. Rheological tests were conducted at 20, 40, and 60 minutes to capture the time-dependent behaviour of the mixtures. The flow spread test evaluated the mortar's consistency and ability to maintain workability over time, essential for continuous extrusion during the printing process. The penetration resistance test assessed the stiffening rate of the mortar, providing insights into setting time and early strength development. The vane and slug tests measured yield stress, a critical parameter for ensuring buildability and layer stability, indicating the mixture's capacity to support subsequent layers without deformation or collapse. The results from the reference mixture were used to compare the performance of mortars with 25% and 50% FRCA content, highlighting the impact of recycled aggregates on time-dependent rheological properties. Mortars containing FRCA exhibited differences in flow retention and yield stress evolution, which are key factors influencing extrudability and printability in additive manufacturing processes.

1 Introduction

The construction industry is constantly modernising, whether through the use of new, more sustainable materials or the adoption of rationalised and automated construction technologies. Aligned with this objective, Three-Dimensional Concrete Printing (3DCP) was introduced to civil engineering in 1998 by Khoshnevis, who presented an additive manufacturing process for cementitious materials known as “Contour Crafting” [1]. Following this, research on this technology in civil engineering gained significance, increasing significantly from 2016 onwards and continuing to show a growing tendency.

The technique essentially consists of extruding overlapping layers of mortar into pre-defined shapes based on computational modelling. Compared to conventional construction methods, 3DCP has the potential to reduce raw material waste, waste generation, construction times, workforce requirements, and indirect costs associated with formwork. Additionally, it promotes automation, flexibility, and architectural freedom, while enabling the integration of construction with prototyping, digital simulation technologies, information modelling, and virtual reality [2-6].

However, a key characteristic of 3DCP is the production of mixtures predominantly without coarse aggregates and, consequently, the use of large quantities of fine aggregates and high binder-to-aggregate ratios compared to conventional concrete [7] which tends to increase the consumption of aggregates and binders.

In this context, the use of fine recycled concrete aggregates (FRCA) derived from construction and demolition waste, along with the use of alternative binders (resulting from the partial replacement of cement with additions such as calcined clay, active silica, fly ash, or slags), can be part of the solution to mitigate the impacts of these characteristics inherent to 3DCP [2, 8, 9].

The use of FRCA has various impacts on the properties of the mixtures due to their inherent characteristics. As reported, the use of recycled aggregates in proportions of 25% and 50% improves buildability but reduces the printability window [10]. To maintain the workability of the mixtures within printable ranges, studies indicate the need to adjust the superplasticiser content [11]. In other cases, the literature points to the need to use various additives in combination, such as viscosity modifiers, nano-clays, defoamers, fibres, sodium gluconate, and early strengthening agents (ESA) [12-23]. The techniques for

* Corresponding author: eduardoklsb@gmail.com

evaluating the behaviour of the mixtures are also diverse. In general, studies in the fresh state assess properties such as workability [20], yield stress and thixotropy [22], green strength [12], extrudability, and buildability [24]. In the hardened state, research has focused on the study of porosity [13, 14] or the mechanical strengths of printed materials [15].

Although there are several studies with different tests, there are still no standardised tests specifically for 3D printing. In this regard, this work aimed to carry out an exploratory study in the fresh state to test some adaptations in the operation of different rheological tests with 3D printing mixtures and to identify the 'effect size' of the substitution of 25% and 50% by volume of natural aggregates with recycled aggregates on the properties assessed.

2 Materials and Experimental Methods

2.1 Materials and Mix Design

The materials used to produce the mortars were a mixture of binders and fine aggregates. The binders included CEM II/AL 42.5 R, silica fume, and limestone filler. The cement and limestone filler, are sourced from Portugal, while the silica fume was obtained from a ferrosilicon plant in Spain. The fine aggregates were composed of mixtures of natural and recycled concrete aggregates. The natural aggregate is river-sourced and siliceous, whereas the recycled concrete aggregates were obtained from a concrete recycling plant in central Portugal, through the crushing of demolition concrete waste and the separation of fine aggregates up to 4 mm. After this initial separation, both the natural and recycled aggregates were dried and sieved to create particle size distributions between 0.063 and 2 mm, according to EN 933-1, as shown in Figure 1.

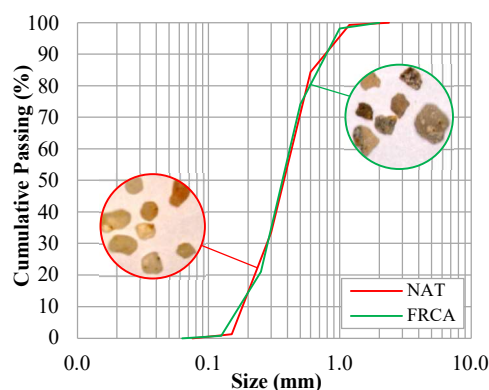


Fig. 1. Particle size distribution of aggregates

The maximum particle size of 2 mm for the aggregates was determined by the limited space between the rotating screw and the stator, such that particles larger than 2 mm could damage the equipment. Physical characterisation tests of the aggregates were also conducted to assist in interpreting the effects of their properties on the rheological behaviour of the mortars. Tests for densities and water absorption (EN 1097-6), loose bulk particle density and void volume with and

without compaction (EN 1097-3), and flow coefficient (EN 933-6) were performed. For the loose bulk particle density with compaction test, the aggregates were placed in a container of known volume in three layers of similar height, with each layer receiving 25 light blows with a steel rod weighing 156 ± 1 g, 0.9 ± 1 cm in diameter, and 30 ± 1 cm in length. Table 1 presents these properties of the aggregates.

Table 1. Properties of natural and recycled aggregates

Property	NAT	FRCA
Oven-dried particle density (kg/m ³)	2631	2262
Satur. surface-dried particle density (kg/m ³)	2637	2420
Water Absorption 24h (%)	0.23	6.97
Compressed Loose Bulk Density (kg/m ³)	1638	1451
Uncompressed Loose Bulk Density (kg/m ³)	1519	1320
Compressed Voids (%)	37.8	35.9
Uncompressed Voids (%)	42.3	41.7
Flow Coefficient Test (s)	27.5	32.8

As shown in Figure 1, it was also observed that the recycled aggregates have a more angular shape, while the natural aggregates are more rounded, a fact explained by the methods used to obtain these materials. Furthermore, the recycled aggregates are more heterogeneous in composition, consisting of fragments of hardened paste and fine aggregates, which partly explains the difference in their properties, particularly their high-water absorption.

In addition, a superplasticiser (water-reducing additive) was used to maintain the consistency of the mixtures within a printable range. The water/binder ratio was the same for all mixtures, set at 0.2. Three mixtures were produced with different levels of natural aggregate substitution by recycled aggregates, as shown in Table 2. All replacements were made to maintain constant the ratio between the paste volume and the aggregate volume.

Table 2. Mix design (kg/m³)

M	C	LF	SF	NAT	FRCA	W	WA	SP
NAT	775	145	80	1075	0	200	0	14.66
R25	775	145	80	806	242	200	16.9	15.98
R50	775	145	80	538	484	200	33.7	16.66

M: mixture; C: cement; LF: limestone filler; SF: silica fume; NAT: natural aggregates; FRCA: recycled aggregates; W: effective water; WA: water absorption; SP: superplasticizer

For the rheological tests, the materials were mixed in a 5L roto-orbital mixer. For the evaluation of extrudability and buildability, due to the need for a larger volume for printing the cylinders, a 35L rotary mixer was used, as shown in Figure 2.



Fig. 2. Mixers (a) 5L (b) 35L

Two different mixing methods were used, as shown in Table 3. Method A was employed for the reference mixture and consisted of manually mixing the dry materials, adding the water, and performing alternating stages of mixing and pauses for scraping the bowl. For the mixtures with recycled aggregates, due to their high water absorption, Method B was used. It includes a preliminary step of manually mixing the aggregates with the absorption water.

Table 3. Mixture Methods

Method A – REF			
Step	T (min)	Procedure	Speed
1	01:00	Sand + binders + 90% water - Mixture	Low
2	01:30	SP + 10% water - Mixture	Low
3	01:30	Stop and scraping	Stop
4	02:00	Mixture	High
5	01:30	Stop and scraping	Stop
6	02:30	Mixture	Low
Total	10:00		
Method B – R25, R50, R100			
Step	T (min)	Procedure	Speed
1	- 02:00	Sand + absorption water FRCA	Manual
2	01:00	Binders + 90% water - Mixture	Low
3	01:30	SP + 10% water - Mixture	Low
4	01:30	Stop and scraping	Stop
5	02:00	Mixture	High
6	01:30	Stop and scraping	Stop
7	02:30	Mixture	Low
Total	10:00		

After mixing, the mortars were placed in sealed containers and maintained in an environment with a temperature of $25 \pm 5^\circ\text{C}$ and a relative humidity of $60 \pm 5\%$ until the testing periods.

2.2 Experimental Methods

The experimental campaign was divided into rheological tests, extrudability and buildability tests, and mechanical tests, as shown in the diagram in Figure 3. To understand the behaviour of the mixtures over time, the rheological tests were carried out at ages of 20 min, 40 min, and 60 min, measured from the mixing of water with the binders. Due to their thixotropy, the mixtures were manually homogenised with a spatula before each test. At the end of the tests, the mixtures were reconditioned in sealed containers until the next testing age.

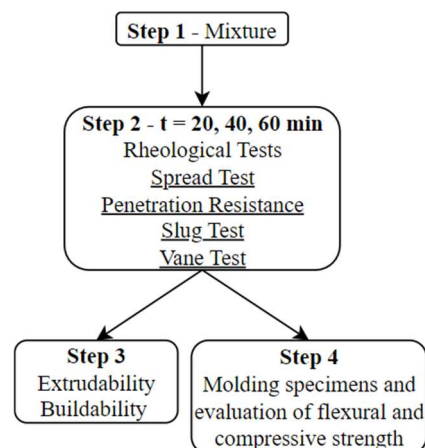


Fig. 3. Method diagram

2.2.1 Spread test

The spread was evaluated according to EN 1015-3, as shown in Figure 4. After moulding the truncated cone, the mould was removed and 15 taps were applied within 15 seconds. The spread reading was the average of 3 measurements taken with a calliper.



Fig. 4. Spread test

2.2.2 Penetration resistance

The penetration resistance was evaluated using an adapted Vicat apparatus for assessing normal consistency according to EN 196-3, as shown in Figure 5. Based on preliminary tests, it was observed that due to the thixotropy of the mixtures, it was not possible to obtain readings with the standard plunger of the standard, as the penetration was always maximal. To address this issue, a $\varnothing 20$ mm epoxy resin plunger was manufactured to increase the contact area and reduce the stress between the weight of the rod with the plunger and the mixture during the test. The total weight of the penetration assembly (rod + plunger) was 309.41 g. After placing the material in the standard mould, the reading was standardised to be taken 30 seconds after releasing the assembly, to allow the displacement to cease.

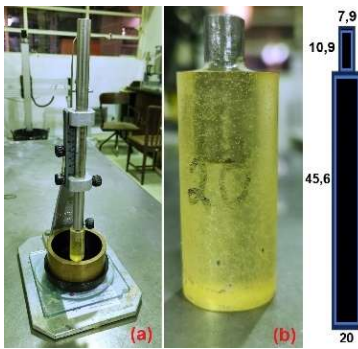


Fig. 5. Penetration test (a) Vicat apparatus (b) plunger

2.2.3 Vane test

This test was performed with a Torvane pocket vane test, a portable device that indicates the shear stress based on the torque required to rotate the blades when inserted into the mortar, as shown in Figure 7. To increase the sensitivity of the equipment, a sensitive adapter with a diameter of Ø48 mm was used.



Fig. 6. Vane test (a) apparatus (b) sensitive vane adaptor

2.2.4 Slug test

The slug test is a method used to obtain the yield stress of the mixtures simply and rapidly. The testing equipment is a prototype built based on a previous study [25] and consists of inserting approximately 500 ml of the mixture into a tube and applying pressure to the material, causing it to exit through a Ø10 mm diameter hole. As the material exits, it forms 'slugs' (small pieces) that fall when the weight force overcomes the cohesive forces of the mixture. Over time, as the material's consistency decreases and cohesion increases, the pieces become larger and heavier. The test is based on the fact that 3D printing mixtures can be considered non-Newtonian fluids, and their behaviour can be estimated using the Herschel-Bulkley model. After some simplifications, the calculation of the flow stress can be performed using Equation 1.

$$\tau_s = \frac{g}{\sqrt{3} \cdot S} \cdot m_s \quad (1)$$

- $\tau_s \rightarrow$ slug test yield stress (Pa)
- $g \rightarrow$ earth gravitational constant (9,81 m/s²)
- $S \rightarrow$ nozzle area (m²)
- $m_s \rightarrow$ average slug mass (kg)

Figure 6 shows the equipment and an example of the test being conducted.

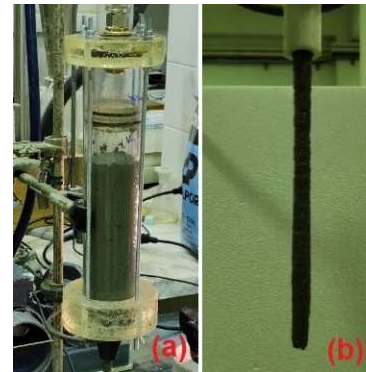


Fig. 7. Slug test (a) apparatus (b) slug

For each mixture, the mass of 30 slugs was weighed. At the beginning of the test, it is common for the first slugs to have defects until the pressure is adjusted. Therefore, the mass of the first 5 slugs was disregarded, and the flow stress calculation was based on the average mass of the last 25 slugs. At the ages of 40 and 60 minutes, for some mixtures, it was not possible to collect 30 slugs because the material did not flow through the hole during the test. In these cases, the mass of the first 5 slugs was discarded, and the calculation was based on the average of the remaining slugs.

2.2.5 Extrudability and Buildability

Extrudability and buildability were assessed based on a cylinder modelled in G-Code in a helical shape, extruded with a screw pump, and printed with a gantry-type 3D printer, as shown in Figure 8. Parameters such as total printed height, average layer height, and average layer thickness were evaluated.

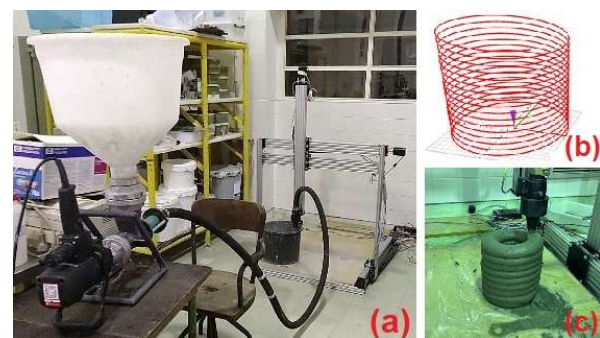


Fig. 8. 3D printer (a) pump and printer (b) sliced g-code (c) printed cylinder

2.2.6 Flexural and Compressive Strength

The flexural and compressive strength of the mixtures were carried out according to EN 196-1. In 3D printing, it is important to understand the development of strengths at early ages, as the layers are continuously overlaid without allowing time for them to reach the design strength. Therefore, specimens were moulded and tested at 1 day, 4 days, 7 days, and 28 days.

3 Results and Discussion

3.1 Spread test

Figure 9 presents the spread test results of the mixtures at ages 20, 40, and 60 minutes.

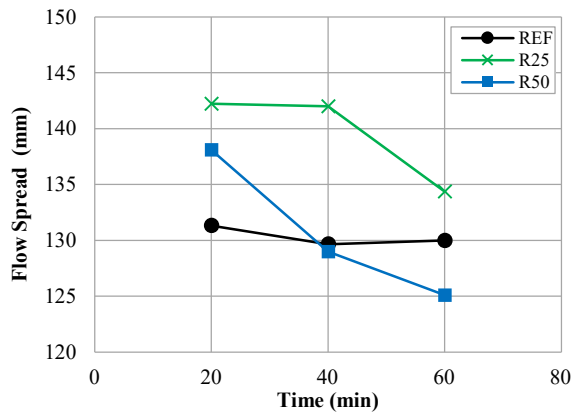


Fig. 9. Flow Spread results

Different behavioural tendency was observed between the three mixtures. The initial hypothesis was that workability would decrease over time due to the loss of superplasticiser action. However, this tendency was not observed in the reference mixture. Even after 60 minutes, the decrease in spread was insignificant. In terms of extrudability for 3D printing, this result is important, as the printing window depends on the maintenance of workability for enough time to extrude the material through the pump.

For the mixtures with recycled aggregates, workability decreased over time, as expected. The spread values of R50 were lower than R25 at all ages, which can be explained by the higher presence of recycled aggregates. Therefore, the behaviour of the mixtures is more influenced by the properties of these materials, particularly their high-water absorption and the more angular shape of the particles.

In summary, the workability of REF did not change over time, but it had the lowest values at 20 minutes. For the mixtures with recycled aggregates, R50 showed the greatest tendency to lose workability over time, while R25 was intermediate, these trends are expression of the progressive absorption of free water by the recycled aggregates.

As previously mentioned, the reference mixture is extrudable and buildable. Therefore, it can be concluded that between 20 and 40 minutes, all the mixtures have the potential to exhibit similar behaviour. However, at 60 minutes, the significant decrease in workability of R50 may compromise its extrudability by causing blockages in the rotor-stator assembly or the pipe passage.

3.2 Penetration resistance

Figure 10 presents the results of the modified needle penetration depth at 20, 40, and 60 minutes. In this test, greater penetration depths indicate lower resistance to movement and, therefore, lower yield stress.

Unlike the spread test, the hypothesis of a decrease in the penetration depth of the plunger over time was confirmed for all mixtures. However, as in the previous test, the R25 mixture exhibited the highest penetration values, indicating it was the most workable for all ages.

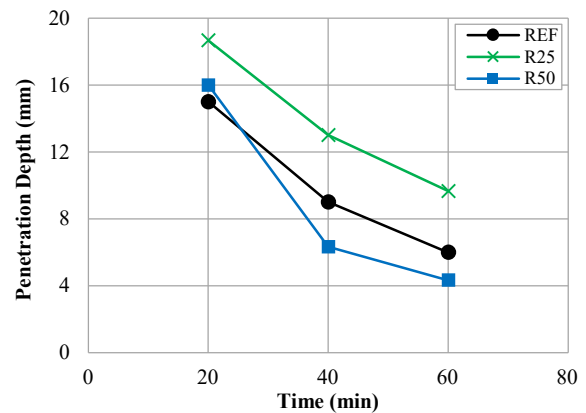


Fig. 10. Penetration depth results

The difference between the results of the reference mixture and R50 at 20 minutes was minimal, but over time this difference increased, particularly at 40 minutes. Therefore, the penetration resistance of the mixtures indicates the same tendency observed in the spread test. Between 20 and 40 minutes, the mixtures are potentially extrudable and printable, but at 60 minutes, the loss of workability may prevent the use of the mixture, especially for R50.

3.3 Vane test

Figure 11 presents the shear stress of the mixtures at 20, 40, and 60 minutes.

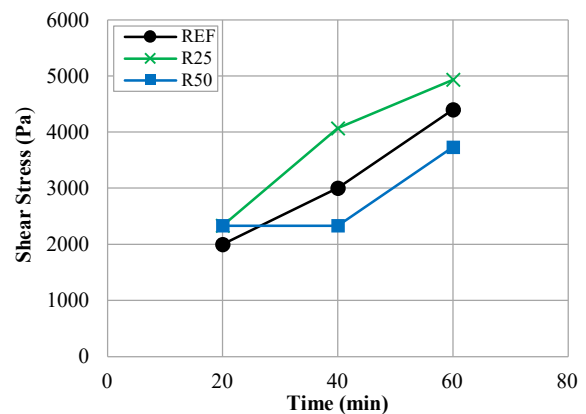


Fig. 11. Vane test results

In this test, the hypothesis is that the shear stress of the mixture can be correlated with extrudability so that over time, the loss of workability is caused by an increase in shear stress. Consequently, the force required for the extrusion (flow) of the material is higher.

The results showed a tendency similar to what was observed in the penetration resistance test. At 20 minutes, the mixtures had similar values that increased over time. However, for the R50 mixture, the values

were the lowest and practically unchanged between 20 and 40 minutes but increased from 40 to 60 minutes. However, it was expected that the R25 mixture would exhibit the lowest shear stress values, as the results from the other tests showed it to have greater workability. Yet, the observed behaviour was the opposite. A possible explanation for this is that the equipment used measures the yield stress only in the top 5 mm of the sample, which may not be representative of the entire mixture. In this space, there is a higher probability of water loss through evaporation.

3.4 Slug test

Figure 12 presents the yield stress results calculated based on the slug test at 20 and 40 minutes. Unlike the other rheological tests, none of the mixtures passed through the extrusion duct at 60 minutes of age, so no readings were taken at this age. However, this behaviour supports the findings from the other rheological tests, where at 60 minutes, the loss of workability can render the mixtures unsuitable for 3D printing.

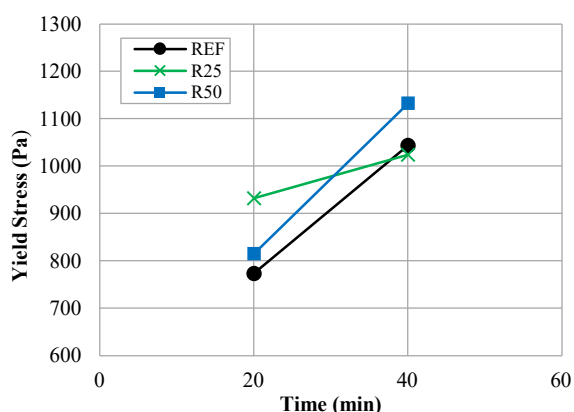


Fig. 12. Slug test results

The results also showed that the R50 mixture exhibited the highest yield stress values at 40 minutes. Therefore, based on the continued increase in yield stress up to 60 minutes, it can be concluded that, as demonstrated in the other tests, this mixture is the most likely to experience extrusion problems at this time.

It can be concluded that considering that the mixtures did not extrude in the slug test at 60 minutes and considering that the reference mixture is extrudable between 20 and 40 minutes, the mixtures with recycled aggregates are potentially extrudable between 20 and 40 minutes. However, after this time, all mixtures may lose their extrudability and become unfeasible for use.

3.5 Extrudability and Buildability

Based on the results of the rheological tests, the printing planning for the mixtures was developed, taking into account the following points:

- The total time required to mix all the batches is 10 minutes;

- The maximum printing window is around 40 minutes;
- For mixtures with recycled aggregates, the loss of workability is more evident, therefore, the printing window may be smaller than expected.

Due to the need for a larger volume to print the cylinders ($\pm 6L$), the mixtures were prepared in the 35L mixer. During the mixing process, the following difficulties were identified:

- Due to differences in the mixing energy and the type of blade rotation, the 35 L mixer requires more time to homogenise the materials, which reduces the printing window;
- It is necessary for the stages (mixing, transport, insertion into the pump, extrusion, and construction) to be highly coordinated to avoid excessive water loss due to evaporation;
- Due to the thixotropy of the mixtures, while the material waits to be inserted into the pump, it is necessary to periodically add mixing energy to keep the material workable, which is difficult to achieve manually.

Despite the observed issues, one cylinder of each mixture was printed between 25 and 45 minutes, demonstrating that the rheological tests conducted have the potential to assess the extrudability and buildability of the mixtures. After extrusion, the buildability was assessed by measuring the total height, external diameter, and layer dimensions with a calliper, as shown in Figure 13.



Fig. 13. Buildability (a) height (b) diameter (c) layer width (d) layer thickness

For printing the cylinders, the following configurations were adopted for the pump and the printer:

- Extrusion flow rate: 8.3 cm³/s
- Printing speed: 0.83 cm/s
- Nozzle diameter: 2 cm
- Pipe diameter: 2.5 cm
- Pipe length: 200 cm

The evaluated parameters are presented in Table 4. The measurements of quantity, width, and thickness of the layers are approximate average values, considering that the printing code used consisted of circles printed with continuous helical increments.

Table 4. Buildability parameters

M	H (cm)	D (cm)	N	W (cm)	T (cm)	V (L)	ρ (kg/m ³)
REF	26.05	18.00	16	4.80	1.63	4.86	2297
R25	26.70	18.55	15	5.77	1.78	5.91	2233
R50	25.30	16.90	16	4.00	1.58	3.89	2204

H: height; D: external diameter; N: layers; W: width; T: thickness; V: volume; ρ : specific density

Figure 14 shows the cylinders printed in profile and top view. It can be observed through the measured parameters and the images that the buildability of the mixtures is different. As expected, due to the angular shape of the recycled aggregates and their higher water absorption, the R25 and R50 mixtures maintain the layer dimensions better after extrusion through the nozzle, meaning there is less deformation after the accumulation of subsequent layers. This is evidenced by the differences in the thickness and width of the layers. However, despite the R50 mixture presenting some local defects, these differences did not cause significant issues that prevented the continuation of printing. Therefore, the only consequence of the differences in the buildability of the mixtures was related to the printed volume, in that with less deformation, less mortar volume per layer was needed to reach the total height.

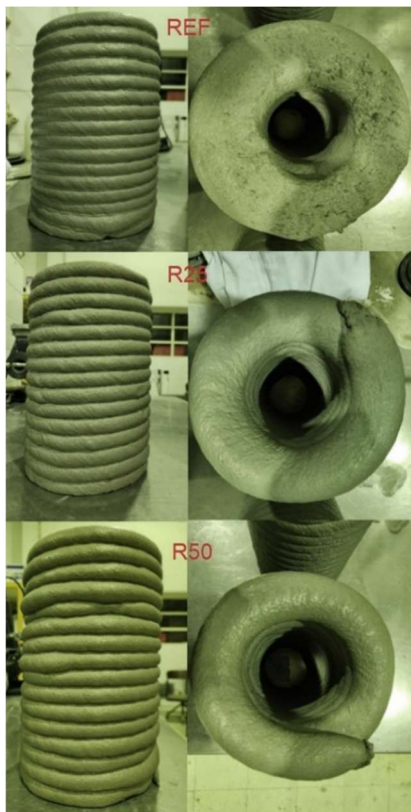


Fig. 14. Visual appearance of printed cylinders

3.6 Flexural and Compressive Strength

The literature shows that the strength of printed specimens is generally lower than that of moulded specimens due to the insertion of voids in the mixture during extrusion. However, extracting printed specimens is more difficult to perform representatively and was not the primary aim of this study. Therefore, conventional specimens were moulded for flexural and compressive strength tests to obtain an indication of the real printed strength and to observe the differences in the development of these strengths between the mixtures studied.

Figure 15 presents the flexural strength of the mixtures at 1 day, 4 days, 7 days, and 28 days of age. In general, at all ages, the flexural strengths of the mixtures with recycled aggregates tend to be lower than those of the reference mixture. The main explanation for this is that recycled aggregates are composed of fragments of hardened mortar, which are more porous than siliceous natural aggregates and, therefore, less resistant.

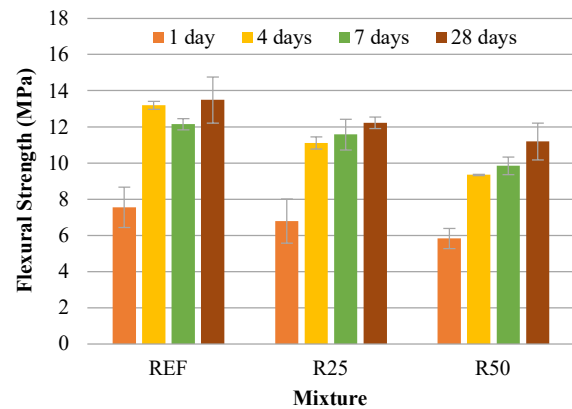


Fig. 15. Flexural strength of mixtures

Most of the flexural strength for all mixtures develops within the first 7 days due to the presence of silica fume, which accelerates the chemical hydration reactions of the clinker. The presence of this pozzolanic material also partly explains the evolution of compressive strength, as shown in Figure 16.

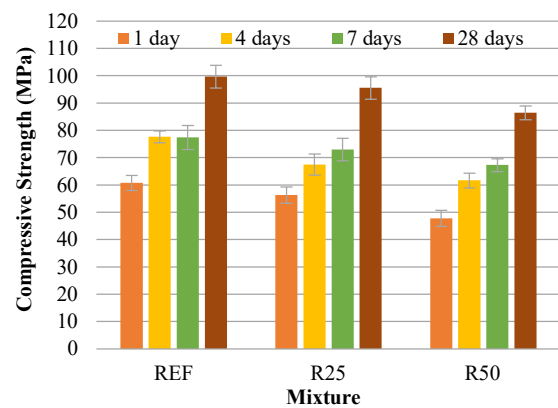


Fig. 16. Compressive strength of mixtures

At 1 day of age, the mixtures already achieve strengths close to high-performance concretes, even for the mixtures with recycled aggregates. This is primarily due

to the low water/cement ratio and the use of pozzolanic materials in the mixture, which refine the microstructure and promote higher strengths. The high strength of the mixtures at an early age is particularly interesting for 3D printing technology, as being buildable during the printing process, must also be moved at early ages as most printed element may be pre-casted and transported away.

In general, it can be concluded that, although lower than those of moulded specimens, the strengths of the printed mixtures are likely still far superior to conventional materials. Additionally, the use of up to 50% recycled aggregate replacement may lead to a decrease of the mixtures compressive strength up to 15%.

4 Conclusions

This study aimed to conduct an exploratory investigation into the rheological parameters, extrudability, buildability, and flexural and compressive strengths of potentially printable mixtures incorporating different percentages of recycled fine concrete aggregates (FRCA). The conclusions were as follows:

- The rheological tests indicated that between 20 and 40 minutes all mixtures have the potential to be extrudable and constructible. After 40 minutes, the mixtures begin to lose workability, increasing the likelihood of rotor-stator blockage in the pump;
- Among the R25 and R50 mixtures, the R25 mixture has the greatest potential for 3D printing use, as the rheological tests indicate adequate workability and sufficient open time for printing. Its extrudability and buildability are similar to the reference mixture, and the strengths are not significantly affected by the properties of the FRCA;
- For the R50 mixture, 3D printing is possible if precautions are taken not to exceed the 40-minute mark. After this period, the loss of workability becomes significant and may compromise extrusion capacity through the pump. However, the buildability of the R50 mixture was the best among the mixtures studied, showing the least deformation of the layers and the best shape retention after layer accumulation;
- The strengths of the 3D printing mixtures are decreased by the introduction of recycled aggregates up to a 50% replacement ratio, keeping high levels, as the water/cement ratio in these mixtures is low, and in general, pozzolans and fillers are used, which improve the strength of the hardened materials;
- Finally, this study demonstrates that the tests used can predict the behaviour of potential mixtures for 3D printing. Moreover, these tests can be used to establish parameter ranges for potentially printable materials, thus facilitating research for the

introduction of new types of materials and more sustainable mixtures.

Acknowledgements: The authors thank National Laboratory in Civil Engineering (LNEC) and Sustainable Construction Materials Association (c5Lab), for their support in developing the research.

Funding: This research was funded by Fundação para Ciência e Tecnologia (FCT), Project “RE-CYCL3D—Recycled Aggregates for 3 Dimension Printed Concrete Structures” reference ERA-MIN3/0002/2021.

Author contribution statement: Conceptualization, E.K.S., and K.F.S.; methodology, E.K.S., and K.F.S.; formal analysis, E.K.S., K.F.S., M.G.V., S.P.S., and B.M.T.; investigation, E.K.S., K.F.S., S.P.S.; writing — original draft preparation, E.K.S.; writing — review and editing, E.K.S.; K.F.S., M.G.V., S.P.S., and B.M.T. All authors have read and agreed to the published version of the manuscript.

References

1. B. Khoshnevis, Automated construction by contour crafting - related robotics and information technologies, *Automation in Construction* 13(1) (2004) 5-19.
2. G. Bai, L. Wang, G. Ma, J. Sanjayan, M. Bai, 3D printing eco-friendly concrete containing under-utilised and waste solids as aggregates, *Cement and Concrete Composites* 120 (2021).
3. B. Panda, S.C. Paul, N.A.N. Mohamed, Y.W.D. Tay, M.J. Tan, Measurement of tensile bond strength of 3D printed geopolymers mortar, *Measurement* 113 (2018) 108-116.
4. C.M. Rouhana, M.S. Aoun, F.S. Faek, M.S. Eljazzar, F.R. Hamzeh, The Reduction of Construction Duration by Implementing Contour Crafting (3d Printing), 22nd Annual Conference of the International Group for Lean Construction, Oslo, 2014.
5. H. Yang, J.K.H. Chung, Y. Chen, Y. Li, The cost calculation method of construction 3D printing aligned with internet of things, *EURASIP Journal on Wireless Communications and Networking* 2018(1) (2018).
6. J. Zhang, J. Wang, S. Dong, X. Yu, B. Han, A review of the current progress and application of 3D printed concrete, *Composites Part A: Applied Science and Manufacturing* 125 (2019).
7. P. Sikora, M. Chougan, K. Cuevas, M. Liebscher, V. Mechtcherine, S.H. Ghaffar, M. Liard, D. Lootens, P. Krivenko, M. Sanytsky, D. Stephan, The effects of nano- and micro-sized additives on 3D printable cementitious and alkali-activated composites: a review, *Applied Nanoscience* 12(4) (2021) 805-823.
8. S. Bhattacharjee, A.S. Basavaraj, A.V. Rahul, M. Santhanam, R. Gettu, B. Panda, E. Schlangen, Y. Chen, O. Copuroglu, G. Ma, L. Wang, M.A. Basit Beigh, V. Mechtcherine, Sustainable materials for

- 3D concrete printing, *Cement and Concrete Composites* 122 (2021).
9. D. Dey, D. Srinivas, B. Panda, P. Suraneni, T.G. Sitharam, Use of industrial waste materials for 3D printing of sustainable concrete: A review, *Journal of Cleaner Production* 340 (2022).
 10. T. Ding, J.Z. Xiao, F. Qin, Z.H. Duan, Mechanical behaviour of 3D printed mortar with recycled sand at early ages, *Construction and Building Materials* 248 (2020) 11.
 11. A.V. Rahul, M.K. Mohan, G. De Schutter, K. Van Tittelboom, 3D printable concrete with natural and recycled coarse aggregates: Rheological, mechanical and shrinkage behaviour, *Cement & Concrete Composites* 125 (2022) 13.
 12. S. Zou, J.Z. Xiao, T. Ding, Z.H. Duan, Q.T. Zhang, Printability and advantages of 3D printing mortar with 100% recycled sand, *Construction and Building Materials* 273 (2021) 6.
 13. Y.W. Wu, C. Liu, H.W. Liu, G.L. Bai, Y.S. Meng, S.M. Ding, Mechanism of the influence of multi-scale pore structure on the triaxial mechanical properties of 3D printed concrete with recycled sand, *Cement & Concrete Composites* 152 (2024) 17.
 14. Y.W. Wu, C. Liu, G.L. Bai, H.W. Liu, Y.S. Meng, Z.H. Wang, 3D printed concrete with recycled sand: Pore structures and triaxial compression properties, *Cement & Concrete Composites* 139 (2023) 17.
 15. J.Q. Tong, Y.H. Ding, X.W. Lv, W. Ning, Effect of carbonated recycled coarse aggregates on the mechanical properties of 3D printed recycled concrete, *Journal of Building Engineering* 80 (2023) 18.
 16. Z.Y. Lv, J.Z. Xiao, Z.H. Duan, Y.X. Tang, Time-dependent evolution and strength modulation of 3D printed concrete pore structure based on microbial remediation, *Journal of Building Engineering* 79 (2023) 13.
 17. Q. Liu, H.L. Tang, K.L. Chen, B. Peng, C. Sun, A. Singh, J.B. Li, Utilizing CO₂ to improve plastic shrinkage and mechanical properties of 3D printed mortar made with recycled fine aggregates, *Construction and Building Materials* 433 (2024) 15.
 18. H.R. Liu, J.Z. Xiao, T. Ding, Flexural performance of 3D-printed composite beams with ECC and recycled fine aggregate concrete: Experimental and numerical analysis, *Engineering Structures* 283 (2023) 15.
 19. C. Liu, Z.H. Wang, Y.W. Wu, H.W. Liu, T.G. Zhang, X. Wang, W. Zhang, 3D printing concrete with recycled sand: The influence mechanism of extruded pore defects on constitutive relationship, *Journal of Building Engineering* 68 (2023) 19.
 20. B.Y. Li, T. Ding, C.W. Qu, W. Liu, Modification of fresh and hardened properties of 3D-printed recycled mortar by superabsorbent polymers, *Journal of Building Engineering* 95 (2024) 15.
 21. Y.H. Ding, Y.Q. Zhang, Y. Zhao, M.X. Zhang, J.Q. Tong, L.L. Zhu, S.Q. Guo, Impact of pre-soaked lime water carbonized recycled fine aggregate on mechanical properties and pore structure of 3D printed mortar, *Journal of Building Engineering* 89 (2024) 17.
 22. J. De Vlieger, L. Boehme, J. Blaakmeer, J.B. Li, Buildability assessment of mortar with fine recycled aggregates for 3D printing, *Construction and Building Materials* 367 (2023) 10.
 23. Z.Y. Chen, S.T. Yang, Q. Liu, M.Q. Xu, S. Wang, T. Lan, Closed-form fracture model for evaluating crack resistance of 3D printed fiber-reinforced alkali-activated slag/fly ash recycled sand concrete, *Journal of Building Engineering* 86 (2024) 20.
 24. S. Zou, J.Z. Xiao, Z.H. Duan, T. Ding, S.D. Hou, On rheology of mortar with recycled fine aggregate for 3D printing, *Construction and Building Materials* 311 (2021) 10.
 25. N. Ducoulombier, R. Mesnil, P. Carneau, L. Demont, H. Bessaies-Bey, J.-F. Caron, N. Roussel, The “Slugs-test” for extrusion-based additive manufacturing: Protocol, analysis and practical limits, *Cement and Concrete Composites* 121 (2021).